Over-the-air Performance of Spectrally-efficient CDMA Signature Sets

Anu Saji, James Bohl, and Ashwin Amanna
ANDRO Computational Solutions, LLC, Rome, NY, USA

***Abstract*—Military communications face increasingly congested environments requiring spectrally efficient approaches capable of contending with many users and interference. We evaluate the over-the-air performance of recently designed minimum total squared correlation (MinTSC) signature sets compared to maximal length pseudorandom binary spreading sequences (m/PN) under a variety of interference conditions. Pre-calculated MinTSC and PN databases feed into a direct sequence Code division multiple access (DS-CDMA) framework capable of emulating a synchronous multi-user scenario. The framework is constructed in GNU radio and implemented on USRP N210 software-defined radios (SDRs). Packet error rate of a data transfer was measured under varying interference conditions. Signature length, interference profile type and interferer power were varied for both MinTSC and PN signature sets. We address transceiver design and implementation challenges including a two-step acquisition and tracking approach to address the difficulties of preamble synchronization. Under single tone (impulse) interference at the center frequency, MinTSC signature sets experience packet errors primarily on the first signature whereas all PN signatures see errors. Under wide-band interference, individual MinTSC signatures perform more uniformly compared to PN. Understanding of this behavior under varying interference provides the warfighter with greater flexibility to adapt to new conditions and can drive assignment of priority data to specific signatures.**

Keywords—GNU radio, SDR, CDMA.

I. INTRODUCTION

Warfighters must contend with increasingly dynamic spectrum conditions and greater congestion from friendly and adversarial users. CDMA technology provides a mechanism for multi-user transmission in limited spectrum. DS-CDMA employs unique spreading signature sets to differentiate multiple users transmitting at the same time and frequency. DS-CDMA has broad applications to military users, such as the common data link, GPS system, low-orbit satellite communication systems, wireless sensor networks and 3G networks.

Signature set selection impacts performance of DS-CDMA in the presence of interference due to the corresponding power spectral density profiles of individual signatures. We investigate the over-the-air performance of newly developed MinTSC signature sets compared to PN of similar length under varying interference conditions. MinTSC signature sets provide the warfighter with greater flexibility in available combinations of number of users and signature length compared to PN.

Previous work on implementing CDMA system on USRP2 and GNU radio focused on zero correlation zone (ZCZ) signature sets [1]. These signatures enabled tracking of only one peak during synchronization. In contrast, we present a more sophisticated preamble detection and synchronization approach and benchmark MinTSC signature sets against traditional PN sets.

MinTSC codes as in [2] is generated from Hadamard-Walsh codes and hence Hadamard-Walsh codes doesn't serve as a good candidate for performance comparison. The MinTSC database at the time of submission of this paper was limited to $L=16$, hence we decided to stick with $L \leqslant 16$. The only available M-sequence signature sets within the *16* bits upper bound is of lengths *7* and *15*. The intent of this paper is to study the performance of MinTSC signature sets in an actual over the air scenario under single tone and wideband interferences and tailor the performance to the spectral properties of the chosen signature sets. Similar approach can be used for studying signatures of longer lengths. PN sequences especially M-sequences have simpler implementation and could be readily implemented.

The test bed, built in GNU radio uses USRP-N210 SDR emulating synchronous multiple users under nominal and varying interference conditions. Pre-defined CDMA signature set databases enable flexibility in selecting varying number of users and signature lengths. To the best of our knowledge, this is the first over-the-air implementation of MinTSC signature sets.

Transmission performance of a MinTSC and PN signature sets is analyzed under single tone and wide-band interference conditions. Results highlight the different behavior of the signature sets driven by the original power spectral density profiles of individual signatures within the respective code sets. Understanding how these different code sets behave under interference has implications towards dynamic management of warfighter communications. With limited spectrum sensing knowledge, a warfighter can adaptively assign individual signatures to specific data streams based on mission priority.

The structure of this paper is as follows: First, we briefly describe how the MinTSC and PN signature sets are generated. Next, the GNU radio USRP N210 implementation is described highlighting technical hurdles and configuration parameters used in the testing. Test methodology and test cases are described, followed by results and discussion. The paper concludes with summary of further work.

II. BACKGROUND

Performance of CDMA systems is highly dependent on the spreading sequences used in these systems. The multiple access interference (MAI) could become very large if the signature sequences are not carefully selected. This interference is a result of the correlation among users' signature sequences which necessitates the need to select signature sequences with low correlation values. A measure of the MAI in the system is given

This research was supported by University Of Buffalo under subcontract R896394

by total squared correlation (TSC). In view of this problem, new families of signature sequences which achieve minimum TSC bounds were developed [2].

In a DS-CDMA system, each of the K participating users are assigned a unique signature sequence vector $\boldsymbol{s}_k \in \mathbb{C}^L, \|\boldsymbol{s}_k\| = 1, k = 1, 2, \ldots, K$. The signature matrix (signature set) of the system is given by $\mathbf{S} = [\mathbf{s}_1, \mathbf{s}_S, \ldots \mathbf{s}_K]_{L\times K}$. Newly developed signatures sets designed to minimize TSC (MinTSC) have been developed and implemented in this paper [2]. The design of minimum TSC binary antipodal signature sets is as proposed in [2]. A Hadamard matrix of size $N \triangleq 4\lfloor(\max\{K, L\} + 1)/4\rfloor$ where K, L are the input parameters to the design procedure are chosen to perform the matrix transformations. These Hadamard matrix transformations result in underloaded and overloaded signature sets that achieve the optimum TSC bound. In addition to lower TSC values, these signatures sets also support more combinations of K and L leading to greater flexibility in selecting signature set to meet a specific need.

In order to compare the performance of MinTSC set against a commonly used family of spreading sequences, we construct a PN database. In this paper, MinTSC signature sets of L = 15, K = 6 i.e.,$\mathbf{S}_{15\times 6}$ and L = 7, K = 6 i.e.,$\mathbf{S}_{7\times 6}$ are compared with PN signature sets of L = 15, K = 6 i.e.$\mathbf{S}_{15\times 6}$, and L = 7, K = 6 i.e.,$\mathbf{S}_{15\times 6}$ respectively.

The 15×6 and 7×6 PN set is constructed using the generator polynomial $x^4 + x + 1$ and $x^3 + x + 1$ respectively. The TSC values of the 15×6 and 7×6 MinTSC, PN signature sets are 6.13 and 6.61 respectively. Analyzing the power spectral density plots of the signature sets shown in Fig. 1 and 2 reveal that the MinTSC and PN signature sets have unique spectral characteristics.

A notable feature is that the first signature in a MinTSC signature set has its spectral peak at the center frequency. Fig. 1

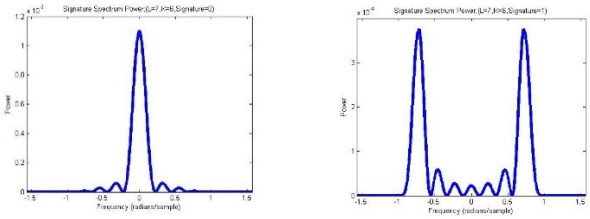

(a) (b)

Fig. 1. Power spectral density of (a) signature 0 and (b) signature 1 of MinTSC signature set where K=6, L=7.

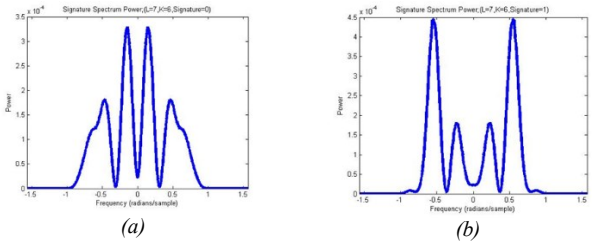

(a) *(b)*

Fig. 2. Power spectral density of (a) signature 0 and (b) signature 1 of PN signature set where K=6, L=7.

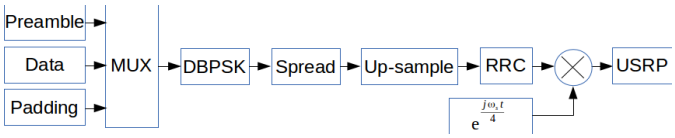

Fig. 3. CDMA Transmitter

shows the power spectral density of signature 0 and signature 1 from a MinTSC signature set where K=6 and L=7 to illustrate the discrete components generated by each signature. In contrast PN signature spectral densities are distributed across the frequency bandwidth more uniformly as in Fig.2. These density profiles are useful in interpreting behavior under interference conditions as discussed in the experimental results section.

III. DS-CDMA ARCHITECTURAL DESCRIPTION

A. CDMA transmitter/receiver

In a CDMA system, multiple simultaneous spectrum users are supported by spreading each user's symbols with a unique signature assigned to that user. This increases the band width of each users signal but allows multiple users to share the same bandwidth. This section describes the transmitter and receiver architecture with specific detail on a two-step acquisition and tracking process for preamble synchronization.

Prior to transmission, data/payload is first broken into packets by breaking the incoming stream into chunks and appending a preamble before the data and a padding bit after the data. The preamble is used at the receiver to synchronize to the CDMA signal. The packetized data stream is then modulated using differential BPSK which drives the need for a padding bit. The resulting symbol stream is then spread using a CDMA spreading signature, as summarized in Fig. 3.

Spreading can be viewed as two operations. First the symbols are up-sampled by a factor equal to the length of the signature, L. To up-sample the signal, L-1 zeros are inserted between each symbol. The second operation is filtering using the spreading signature. This is done using a finite impulse response (FIR) filter with L taps. The taps are the spreading signature values. The next step on the transmitter side is to apply a pulse shaping filter to limit the bandwidth of signal.

The pulse shaping filter used is the Root Raised Cosine (RRC) filter. First, the signal is up-sampled by a factor of 4. Then the RRC filter is applied to the signal. The last step on the transmitter side is to shift the signal spectrum up in frequency so that there is no signal energy at the center frequency. This is done due to local oscillator leakage in the USRP. If the signal was transmitted without shifting, the local oscillator leakage, which would appear as a narrow-band signal at the center frequency, would interfere with the CDMA signal. The shifting moves the signal so it does not overlap the local oscillator leakage signal. A single USRP transmitter can be used to emulate K synchronous users. This is achieved by adding the signals from each user before the RRC filter. The cost for this is reduced signal power for each signature.

Fig. 4 shows a top level diagram of the CDMA Receiver. At the transmitter, the signal was shifted up in frequency before transmission. The first step at the receiver is to shift it back down to center the CDMA signal at 0Hz. Next, the signal is filtered by

a RRC filter. This filter removes any noise outside of the CDMA signal bandwidth and removes the inter-symbol interference caused by the RRC filter at the transmitter. After filtering the signal is sent to separate receivers to receive each signature. Any number of signatures can be assigned to a specific user. In our implementation, we use linear minimum mean squared error multi-user detector (MMSE-MUD) filter coefficients to de-spread the sample stream. This is performed to suppress the effect of MAI on each users' received sample stream.

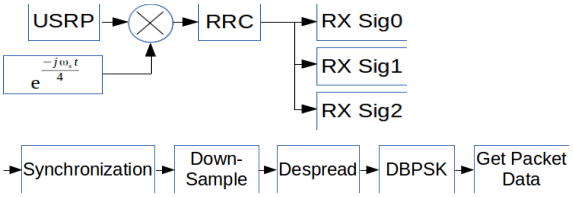

Fig. 4. CDMA Receiver

The first step is synchronization followed by the process of decoding the CDMA signal. This process is essentially the reverse of the encoding. First, the signal is de-spread by filtering the signal using the spreading signature and then re-sampling at the current sample rate divided by L. The sample timing is determined from the synchronization step. The symbols generated by de-spreading are converted to bits by a DBPSK demodulator. Finally the packet data is stripped from the packet. The location of the data in the bit stream is determined by the synchronization step.

B. *Synchronization*

Synchronization is needed to find the optimal sampling point for de-spreading as well as finding the start of the packets. Synchronization locates the precise location of the packet preamble in the received sample stream. Using this location, the start of the packet and the optimal sampling point can be determined. The preamble is a 127 bit Gold sequence. Each user is assigned its own preamble so that the receiver will only be able to synchronize to the user it is looking for.

Synchronization is performed by correlating to the preamble sequence. To reduce the computational requirements of the correlation to allow for a single receiver to receive multiple signatures, the correlation is broken down into two steps, coarse and fine detection. The role of the coarse detection is to find roughly where in the input sample stream the preamble is located. Once this location is found, the fine preamble detection is performed. The computational requirements of the coarse detection have been reduced by not looking for the preamble at all possible sample offsets. This has the disadvantage of missing the preamble some of the time. It may take several packet before coarse detection succeeds. The computational requirements of the fine detection have been reduced by only correlating over a small window of samples. This is possible because the location of the preamble is known based on the coarse detection.

Synchronization is separated into two modes of operation: acquisition and tracking. The acquisition phase performs the coarse detection process first to find the starting sample location of the preamble within a defined threshold. If successful, the tracking phase performs the fine scale preamble detection to identify the exact start of the packet.

1) *Acquisition using coarse preamble detection*

In the acquisition mode, the receiver does not have any information about the location of preamble in the packet. In acquisition mode, the receiver first does a coarse preamble detection to locate a preamble in the received stream within 1 bit as notionally shown in Fig. 5. This coarse detection will not locate every preamble which will result in packets being dropped. After the coarse detection has located a preamble, the receiver will switch to the tracking mode and perform a fine preamble detection.

The coarse preamble detection operates in a stream based mode of operation. Incoming samples are first delayed by a variable number of samples from 1 to 4L. This delay affects the alignment of the incoming sample stream. The delay is incremented by one after a configurable number of samples. Here, the number of samples was equal to 2 times the number of samples in the preamble. Eventually, the sample stream and the de-spread code will align close enough for a preamble to be detected. After the delay block, the signal is down-sampled, de-spread, and DBPSK demodulated to extract a stream of bits. A bitwise sliding correlation is performed on this bit stream to locate the preamble. This correlation counts the number of bit errors between the bit stream and the known preamble. This bit error, currently set to 25 bits, is used to determine when to switch to tracking mode as described previously.

2) *Tracking using fine preamble detection*

The fine preamble detection finds the precise start of the first sample of the first spread bit of the preamble. Starting at the sample provided by the coarse detection, the entire packet, including the preamble, is de-spread and demodulated. A bit error test is performed on the preamble. If the number of bit errors is greater than a threshold, currently 30-40 bits, it is assumed that the coarse acquisition has failed and will change back to acquisition mode. If the bit errors is less than the threshold, the system will remain in tracking mode. In tracking mode, the start of the next preamble is found using a fixed offset from the previous preamble.

The fine preamble detection works by down-sampling, de-spreading, decoding, and correlating with the preamble at all possible time offsets within a 3 bit window, as shown in Fig. 6. The input signal is fed into $(1 + 3 * 4 * L)$ delay lines. In each path, the signal is delayed by 1 from the path above it. In each path, the signal is down-sampled, de-spread, and DBPSK demodulated. Then the preamble bit errors is found and the preamble symbols are correlated. This is performed once for each stream. Finally, the streams with the minimum number of bit errors is found. If there are multiple streams with bit errors equal to the minimum, the stream with the highest correlation is chosen. The output is the delay of the stream that produced the highest correlation given that it had the minimum bit errors. This delay provides the exact start of the preamble with the optimal sampling point.

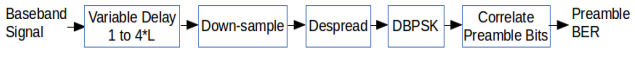

Fig. 5. Coarse Preamble detection

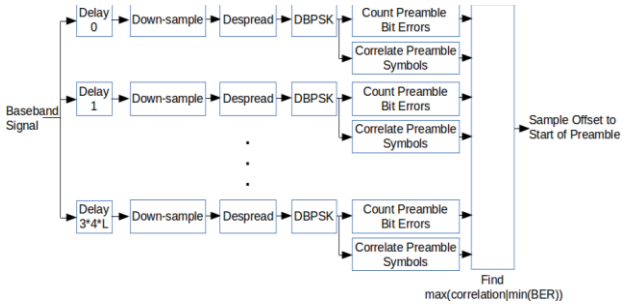

Fig. 6. Fine preamble detection

C. Test bed setup

The system model consisted of three USRP N210s each of which served as a transmitter, receiver and an external interferer respectively. Two laptops operating Linux OS controlled the transmitter and receiver independently while the receiver laptop also operated the GNU radio flow for the interferer. The configuration parameters of the testbed setup; GNU Radio version = 3.7.2.1, UHD driver = 3.7.2, Linux version = Linux Mint 16, USRP = N210, Daughter card = SBX, Center frequency = 915MHz, Sample rate = 500 kS/s, TX power gain = 10dB, Chip rate = 125kS/s, Bit rate = (Chip rate /L) and bandwidth = 125kHz, were set at both laptops. Ten packets of 160 bytes payload were transmitted. Transmit power gain was set to 10dB and the receiver power gain was set to 15dB. A preamble was appended to each payload packet along with a padding bit prior to transmission. No additional buffering was implemented. PER was calculated after the entire data file was transmitted. 10 independent trials of each test were run and averaged together.

During interference scenarios, the external interferer transmitted either a single tone or a wide-band interference signal centered at 915MHz (referred to hereafter as *f0*) simultaneously with data transmission. The wide-band interference signal was 110 kHz wide and was created by band-pass filtering a random stream of data where samples are either 1 or -1 with a probability of ½.

D. Experimental Results

Over-the-air tests were performed on MinTSC and PN signature sets under single tone and wide-band interference conditions. Results from a nominal number of user ($K=6$) and signature length ($L=7$) are shown. Additional tests were performed for $K=6$ and $L=15$. Packet error rates (PER) for each user/ individual signature and for the overall system are measured.

Comparing the performance of $K=6$ MinTSC system at $L=7$ (Fig. 7(c)) and *15* (Fig. 8(c)), it can be seen that the overall PER is < 0.2 for $L=15$ and ≈ 0.2 for $L=7$. Analyzing the individual signatures of $L=7$ (Fig. 7(a)) vs *15* (Fig. 8(a)), it can be seen that longer signature lengths give better resilience to tone interference as only the signature-*0* is affected unlike at $L=7$ where signature-*3* as well is impacted. Also, signature-*0* of $L=15$ doesn't degrade until the tone interferer gain increases to -*21dB* whereas both signature-*0* and *3* of $L=7$ are starting to degrade when tone interferer gain is -*25dB*. Now we compare the $K=6$ M-sequence system at $L = 7$ (Fig. 7(c)) vs *15* (Fig. 8(c)). The signatures of $L=7$ M-sequence system (Fig. 7(b)) starts to degrade for a tone interferer of transmit gain -*25dB* and peaks to *1.0* at -*15dB* whereas the $L=15$ system (Fig. 8(b)) offers more resistance to tone interferer and doesn't degrade until the interferer gain increases to -*7dB*. Unlike $L=7$ signatures the PER doesn't peak to *1.0* and the system PER < 0.1.

Since the spectral component of signature-0 of MinTSC system is at *f0* (refer Fig. 1(a)), a tone interferer at *f0* degrades the signature irrespective of its length. Signature-0 contributes to the overall PER of MinTSC even at $L=15$ (Fig. 8(a)) which is not the case for M-sequence (Fig. 8(b)). Therefore, when comparing the overall PER of MinTSC with M-sequence, we see a significant performance difference. Sig0 of $L=15$ MinTSC is masking the error-resilience exhibited by the rest of the signatures (*1-5*) of the same set which are in fact performing error-free all throughout unlike M-sequence whose signatures starts to degrade at -*7dB*. These individual signature performance under tone interference can be used as a basis for selecting signatures for a system performing in presence of tone interferer at *f0*. For example, if signature-0 of the $L=15$ MinTSC system was not assigned to a user, the system would be performing error-free for tone interferer with transmit gain in the range of -*25dB* to -*5dB* unlike M-sequence system. In general, it was also observed that PN experienced more inconsistent performance as illustrated by the larger error bars in all PN results.

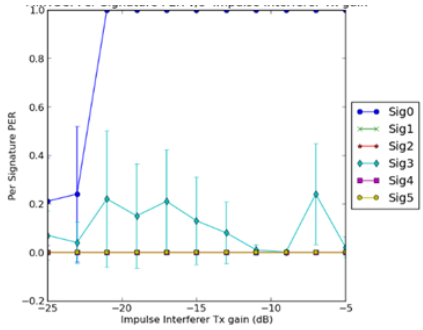

Fig. 7(a) MinTSC per signature PER for K=6 and L=7 in the presence of a single tone interference signal

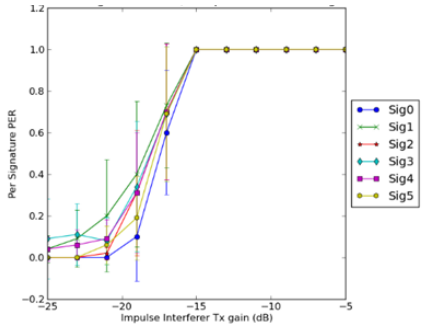

Fig. 7(b).PN per signature PER performance for K=6 and L=7 in the presence of a single tone interference signal

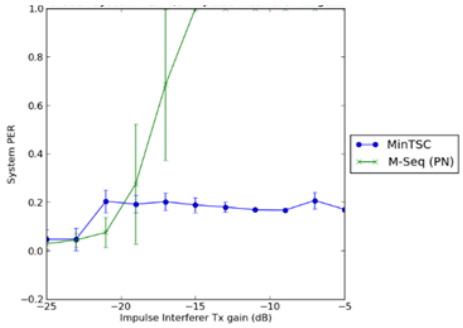

Fig. 7(c).System PER for MinTSC and PN signature sets where K=6 and L=7 in the presence of a single tone interference signal

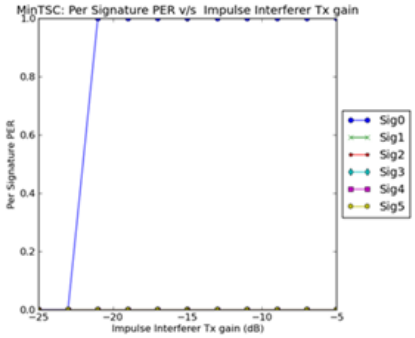

Fig. 8(a). MinTSC per signature PER for K=6 and L=15 in the presence of a single tone interference signal

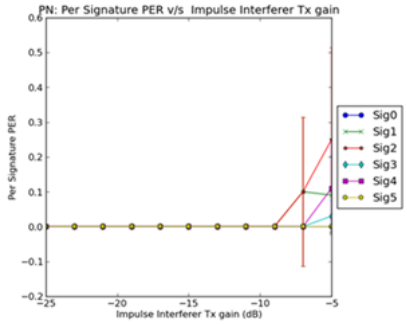

Fig. 8(b). PN per signature PER performance for K=6 and L=15 in the presence of a single tone interference signal

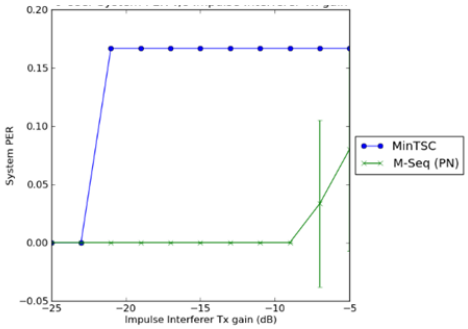

Fig. 8(c). System PER for MinTSC and PN signature sets where K=6 and L=15 in the presence of a single tone interference signal

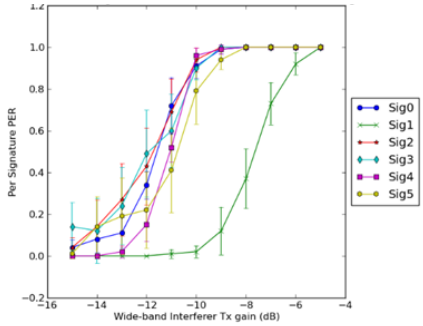

Fig. 9(a). PER for individual signatures of a MinTSC set in the presence of a wide-band interference source where K=6 and L=7

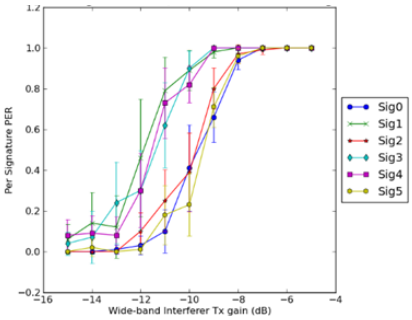

Fig. 9(b). PER for individual signatures of PN set in the presence of a wide-band interference source where K=6 and L=7

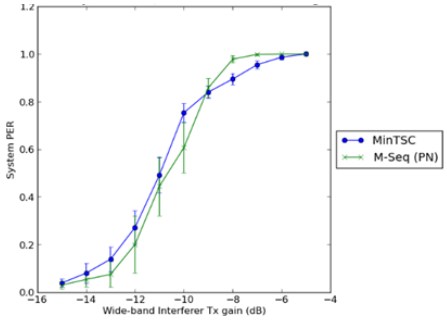

Fig. 9(c). System PER in the presence of a wide-band interference source where K=6 and L=7

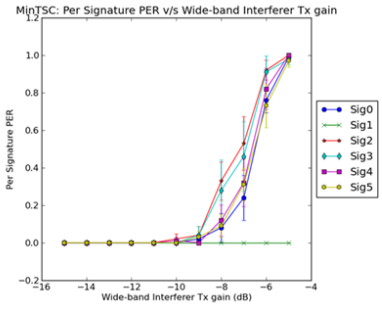

Fig. 10(a). PER for individual signatures of a MinTSC set in the presence of a wide-band interference source where K=6 and L=15

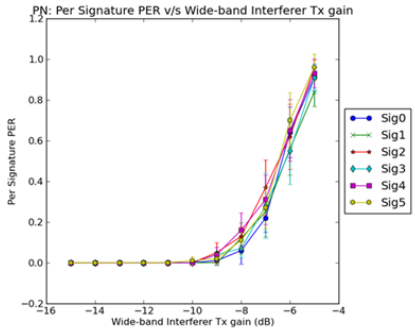

Fig. 10(b). PER for individual signatures of PN set in the presence of a wide-band interference source where K=6 and L=15

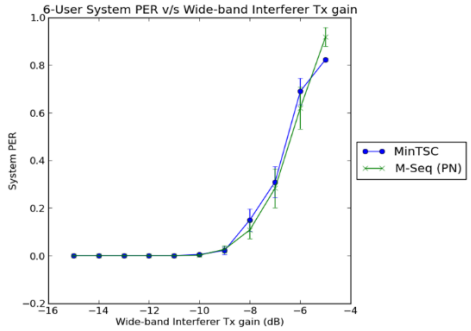

Fig. 10(c). System PER in the presence of a wide-band interference source where K=6 and L=15

The performance of individual signatures of *L=7* MinTSC system as shown in Fig. 9(a) of the paper demonstrates that signature-*1* of the set is comparatively more resilient to wideband interferer till *-10dB* and gets significant errors thereafter. Similarly, examining the individual signature performance of *L=15* MinTSC system reveals error-free performance by signature-1 unlike M-sequence system where all signatures are equally affected. It can be seen that longer signature offers improved resilience to wideband interferer attacks till *-10dB* for both MinTSC and M-sequence systems. The wideband interferer covers the *±0.3454 radians per sample* band of the spectral density plots. We attribute the error-resilience of signature-*1* of MinTSC at *L=7* and *15* to the spectral characteristics of this particular signature which unlike the remaining signatures of the set has its prominent spectral components outside of the *± 0.3454 radians per sample*. From an overall system perspective, both MinTSC and PN at *L=7* and *15* experienced comparatively similar PER, as shown in Fig. 9 and 10(c). This is expected since the wide-band interference covers nearly *80%* of the CDMA bandwidth, and encompasses most of the peak spectral components of each individual signature of both MinTSC and PN signature sets.

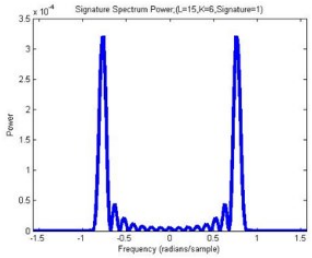

Fig. 11. Power spectral density of signature 1 of MinTSC signature set where K=6, L=15.

IV. Conclusions and Future Work

This paper implemented MinTSC signature sets and benchmarked them against traditional PN codes under various interference scenarios. The implementation featured a unique approach to preamble detection and synchronization. Results indicate that the unique spectral components of individual signatures have bearing on the overall system performance.

Future work can build upon the MinTSC foundation to address aperiodic total squared correlation (ATSC) signature sets to support asynchronous transmitters [3]. In addition to developing new signature sets, effort is needed to improve multi-user detection processes. Other potential efforts include implementing iterative algorithms ("auxiliary-vector") for estimating minimum-variance-distortion-less-response (MVDR) filters to support improved preamble detection that do not require computationally expensive matrix inversions [4]. Finally, these efforts would culminate in developing fully adaptive signature sets to meet changing spectral conditions [5].

References

[1] M. Gandhi and P. Kumar, "GNU Radio + USRP2 Implementation of a Single-Carrier Zero-Correlation-Zone CDMA System," Master's thesis, KTH Information and Communication Technology, Stockholm, Sweden, 2013.

[2] G. Karystinos and D. Pados, "New Bounds on the Total Squared Correlation and Optimum Design of DS-CDMA Binary Signature Sets," *IEEE Transactions on Communications*, vol. 51, pp. 48–51, 2003.

[3] H. Ganapathy, D. Pados, and G. Karystinos, "New Bounds and Optimal Binary Signature Sets - Part ii: Aperiodic Total Squared Correlation," *Communications, IEEE Transactions on*, vol. 59, no. 5, pp. 1411–1420, May 2011.

[4] D. Pados and G. Karystinos, "An Iterative Algorithm for the Computation of the MVDR Filter," *Signal Processing, IEEE Transactions on*, vol. 49, no. 2, pp. 290–300, Feb 2001.

[5] L. Wei, S. Batalama, D. Pados, and B. Suter, "Adaptive Binary Signature Design for Code-division Multiplexing," *Wireless Communications, IEEE Transactions on*, vol. 7, no. 7, pp. 2798–2804, July 2008.